X-690-75-125

PREPRINT

NASA TM X- 70899

SUMMARY OF INITIAL RESULTS FROM THE GSFC FLUXGATE MAGNETOMETER ON PIONEER 11

M. H. ACUNA
N. F. NESS

REVISED

OCTOBER 1975

GSFC — GODDARD SPACE FLIGHT CENTER —
GREENBELT, MARYLAND

SUMMARY OF INITIAL RESULTS FROM THE GSFC FLUXGATE MAGNETOMETER ON PIONEER 11

by

Mario H. Acuña
Norman F. Ness
Laboratory for Extraterrestrial Physics
NASA/Goddard Space Flight Center
Greenbelt, MD 20771

Presented at Tucson Jupiter Meeting 18-23 May 1975
To Be Published in Book Jupiter The Giant Planet ed. by T. Gehrels

May 1975
Revised October 1975

SUMMARY OF INITIAL RESULTS FROM THE GSFC FLUXGATE MAGNETOMETER ON PIONEER 11

Mario H. Acuña
Norman F. Ness
Laboratory for Extraterrestrial Physics
NASA/Goddard Space Flight Center
Greenbelt, MD 20771

ABSTRACT

The main magnetic field of Jupiter has been measured by the GSFC Fluxgate Magnetometer on Pioneer 11 and analysis reveals it to be relatively more complex than expected. In a centered spherical harmonic representation with maximum order n = 3 (designated GSFC model O_4) the dipole term (with opposite polarity to Earth's), has a magnitude of 4.28° Gauss-R_J^3, tilted by 9.6° towards system III longitude of 232 (epoch 1974.9). However, the quadrupole and octupole moments are significant, 24% and 21% of the dipole moment, and this leads to deviation of the planetary magnetic field at distances < 3 R_J from a simple offset tilted dipole. The GSFC model shows a north polar field strength of 14 Gauss, while in the south it is 10.4 Gauss. In the northern hemisphere the "footprint" of the Io associated flux tube passes directly over the polar region. Derived L shell parameters for the radiation belts predict enhanced absorption effects due to the satellites Amalthea and Io as a result of the field distortion. Warping of the charged particle magnetic equator from a plane is also predicted.

Introduction - A high field, triaxial fluxgate magnetometer (FGM) was placed on Pioneer 11 by GSFC to measure the strong planetary magnetic field. A brief note based upon real time, quick-look data obtained during encounter on 3-4 December 1975 reported the discovery of a distorted main magnetic field of the planet with significant quadrupole and octupole contributions (Acuna and Ness, 1975b). A subsequent analysis of the data based upon a more comprehensive data tape, improved spacecraft attitude and A/D converter performance information and comparisons with charged particle data has allowed a more accurate determination of these higher order moments and their consequences for charged particle motion and absorption effects associated with the natural satellites Io and Amalthea.

It is the purpose of this report to elaborate on the FGM results and their implications for the study of trapped particles, planetary radio emissions and planetary interiors.

Instrumentation - The FGM provides instantaneous triaxial vector measurements of the 3 components of the magnetic field using a 10 bit precision A-D converter. The maximum measurable field is 10 Gauss along each orthogonal axis and the quantization step size is $\pm 600\gamma$ for field intensities less than 2 Gauss. Measurements are made once every 36 seconds in an inertial reference frame synchronized with the rotation of the spacecraft ($T_{S/C}$ = 12 sec.). Data digitized by the instrument are sent directly to ground without further processing.

The instrument is extremely light weight (0.272 kgm) and uses only 0.3 watts of power (provided by the GSFC Cosmic Ray Telescope Experiment).

A view of the FGM instrument is shown in Figure 1. Two identical ring core sensors, mounted perpendicular to each other, provide 4 measurements of 4 orthogonal axes, of which 2 are identical. The sensors were so oriented as to provide a redundant measurement of the magnetic field component parallel to the spin axis of the spacecraft. The analog signal from the redundant Z-axis of the 2nd sensor was digitized by the Pioneer spacecraft 6 bit A-D converter and its value transmitted at the same rate as the primary vector measurements.

Although no sensitivity calibrations of the magnetometer were performed in flight, no drift of the systems zero levels were noted from pre- and post-encounter measurements in the weak interplanetary field. Since the output of each axis is biased to 1/2 of the A-D converters dynamic range, this provided direct verification of the A-D converters calibration.

The redundancy provided by the dual Z-axis measurements was used to monitor the sensitivity calibration of each core versus the other and thus give a measure of the internal consistency of the data. The maximum field measured along the Z-axis was approximately 1 Gauss which represents only 5 quantization steps of the spacecraft's A-D converter. Thus, in the absence of additional information and based on the nominal performance of this converter (±1 count), it was possible to verify the sensitivity calibration to within ±20%. Our preliminary report based on quick-look data (Acuña and Ness, 1975b) is consistent with this sensitivity calibration verification, but subsequent comparisons with charged particle anisotropy directions observed near closest approach (Van Allen; Fillius et al. private communications) indicated the possibility of a slight sensitivity

calibration drift in the X-Z sensor. Very recently three calibration voltages associated with the spacecraft's A-D converter, accurately measured at 3 selected transition points (6%, 50%, 81%) have become available. They allow a more precise intercomparison of the Z-axis data, revealing a 10% sensitivity increase in the X-Z sensor. This small but significant effect is illustrated in Figure 2 where the redundant Z-axis data has been plotted versus the main Z-axis data. The straight lines represent the original and corrected calibrations for the X-Z sensor.

This correction yields excellent agreement with charged particle data obtained by co-experimenters on the spacecraft (Van Allen et al., 1975; Fillius et al., 1975), and good agreement with magnetic field data (Smith et al., 1975). A complete description of the instrument has been published elsewhere (Acuna and Ness, 1975a).

Measurements and Analyses - The triaxial measurements of the magnetic field are corrected for phase and amplitude distortion by the spinning spacecraft and then rotated to a Jupiter centered spherical coordinate system. A total of 685 vector measurements were obtained during the close encounter period, 0120 to 0926, December 3, 1974 corresponding to distances less than 6 R_J. Due to an unfavorable bit rate allocation for this instrument during occultation, no measurements were obtained during that period when the spacecraft was operated in a memory storage mode.

The data have been analyzed in terms of a classical Schmidt normalized spherical harmonic expansion fitted to the observations in a least squares sense. In view of the quantization step size, it is reasonable to neglect external harmonic terms in any such representation, for distances less than 10 R_J. Such terms are associated with the highly distorted distant

magnetosphere of Jupiter, observed at distances greater than 20-25 R_J (Smith et al., 1975). As shown by Acuna and Ness (1975b), the measurements from the GSFC FGM instrument show significant departures from the values expected based upon the offset tilted dipole model (D_2) of the Jupiter field (Smith et al., 1974).

The observations between 1.7 - 6.0 R_J have been fitted in the least squares sense so as to minimize the vector residual to harmonic expansions of the following form;

$$\vec{B} = -\nabla V;\ V = a \sum_{n=1}^{n\ max} \sum_{m=o}^{n} \left(\frac{a}{r}\right)^{n+1} \left(g_n^m \cos m\phi + h_n^m \sin m\phi \right) P_n^m (\cos\theta) \quad (1)$$

The inclusion of quadrupole, and octupole terms leads to a significant reduction in the root mean square deviation of the residuals. An offset tilted dipole (OTD) can be obtained by using 6 of the 8 coefficients in a quadrupole expansion.

Table 1 summarizes results for the dipole moment in all of the GSFC expansions thus far taken. Note the variation in the characteristics of the dipole term as the order of the expansion increases. This variation is an expected phenomenon, due to the cross coupling of harmonic coefficients, in situations such as this in which the data set is not "complete" in a mathematical sense so that a set of mutually dependent coefficients occurs. The comparison of the measured magnetic field with that predicted from the spherical harmonic representations is shown in Figure 3 for the O_4 model. The overall agreement with the observations is excellent in all three components of the field.

It is essential in any such representation to conduct an error analysis to determine the statistical stability of the various coefficient sets. The use of the RMS parameter, while appropriate, is a measure which is not complete. In the general problem of solving a linear set of equations, such as obtained in the minimization of the vector residual, it is also useful to consider the condition number of the matrix to be inverted, regardless of the specific method finally employed to affect a solution. The condition number is related to the ratio of the magnitude of the largest to the smallest eigenvectors of the matrix to be inverted. The smaller the number the better, i.e., more stable, the estimates of the unknowns. Table I shows that the condition number for the O_4 model is quite modest, being only 50 while it would increase to 340 for a hexadecapole model. Inclusion of external terms, such as by Smith et al. (1975), increase the condition number to very high values so that there may exist considerable uncertainty in some of the coefficients so derived. Neither the trajectory uncertainties nor the quantization step size adversely affect the determination of the coefficient set for O_4.

Extrapolation of the magnetic field model to the surface of the planet is illustrated in Figure 4. The magnitude of the field of Jupiter for the O_4 model is shown along with other parameters related to Pioneer 11 and the satellite Io. An important feature of our model is the hemispherical and azimuthal asymmetry in both the surface field and in the field topology which results from the significant values of the quadrupole and octupole moments. Table II summarizes the magnitude and phase of the higher order moments for the quadrupole and O_4 models. The table also includes a computation of the normalized magnitude of the higher order

moments relative to the dipole term. It is seen that in the O_4 model the quadrupole is approximately 24% of the dipole term while the octupole is approximately 21%. These values exceed those of the Earth, which are respectively 14 and 9%.

It is appropriate at this point to consider comparison of this GSFC O_4 magnetic field model with those derived from other instruments on Pioneers 10 and 11. Smith et al. (1974) proposed, on the basis of their Pioneer 10 helium vector magnetometer measurements, that the planetary field was well represented by an offset tilted dipole with moment 4.0 Gauss R_J^3 tilted at 10.6° towards a system III longitude $\lambda_{III} = 222°$ in December 1973. On the basis of charged particle measurements from Pioneer 10, Van Allen et al. (1974) derived a centered dipole tilted 9.5° toward $\lambda_{III} = 230°$ which was reported to better represent the results as measured by radiation belt characteristics. The dipole term in the GSFC O_4 model (tilt = 9.6° and $\lambda_{III} = 232°$) shows good agreement with the Van Allen et al. model but less satisfactory agreement with the Smith et al. (1974) model. (Note λ_{III} computed for 1973.9.)

More recently, Smith et al. (1975) have presented a spherical harmonic analysis in which they report a dipole term possessing a tilt angle of 9.9° and a longitude of 227° while the quadrupole and octupole moments are 20% and 15% of the dipole moment respectively. The GSFC O_4 model is in good agreement with these results, the minor differences being probably due to different procedures and methodologies in mathematical analysis of the data, the number of data points included and the radial distances considered.

Implications: Charged Particles - The motion of charged particles in a planetary magnetic field has been studied extensively only in the case of Earth (see reviews by Schulz, 1974 and West, 1975). In such studies, it has been found necessary to use a high order harmonic representation of the terrestrial field even though the quadrupole and octupole moments are only 14 and 9% of the dipole moment and higher multipoles significantly less. This is because the guiding center of the charged particle cyclotron motion, as it moves from northern to southern mirror points, drifts irregularly in longitude. While on Earth, the electrons drift eastward and the protons westward, charged particle drift motion at Jupiter is opposite because the dipole moment of Jupiter is opposite to that of the Earth.

In initially describing the relative position of the spacecraft trajectory with respect to the planetary magnetic field, it is convenient to utilize the classical L shell parameter which measures (in an appropriately normalized sense) the equatorial distance of the field line about which a charged particle is moving. For charged particles, the equatorial point along the field line is defined where the field intensity is a minimum.

We have calculated the corresponding L values derived from the GSFC O_4 model along the Pioneer 11 spacecraft trajectory and these are shown in Figure 5. Those charged particles which would impact the satellites Io and Amalthea in their complicated cyclotron, bounce and drift motion can be expected to be absorbed by those natural satellites (Mead and Hess, 1973; Hess et al., 1974). We have also computed the corresponding L shells swept out by Io and Amalthea for the O_4 model and

these are included in Figure 5. For Io, the O_4 L values swept out are 6.13 to 5.79, while for Amalthea, the O_4 L values are 2.66 to 2.34. The predictions of magnetic field models for satellite sweeping have met with varied success according to the charged particle instruments on Pioneer 11 (Fillius et al., 1975; Simpson et al., 1975; Trainor et al., 1975 and Van Allen et al., 1975). Part of the difficulty at Io may be associated with the demonstrated existence of a source of charged particles observed near this satellite (McIlwain and Fillius, 1975).

A more complete treatment of particle drift shells-pitch angle distributions and individual detector energy-angle characteristics is necessary in order to fully study these problems of satellite sweeping. Here only the simplest view has been taken: that of geometrical sweeping of particles and without proper consideration of the differences of L with pitch angle (at the satellites and at Pioneer 11).

The situation at Amalthea is interesting because of the complex nature of the radiation belt structure observed there by Pioneer 11 (Fillius et al., 1975). Figure 6 presents a comparison of expected absorption effects associated with Amalthea predicted by two models of the planetary field: D_4 (Smith et al., 1975), and O_4 with the observations by Pioneer 11. It is seen that the O_4 model provides a better correspondence of the observed characteristics of minima and maxima of the multiple peak radiation belt structure close to the planet. This provides a completely independent but very powerful test which endorses the physical validity of the O_4 model. However a completely satisfactory explanation of the observed structure is still lacking. It should be noted that with larger multipole moments the complexity of charged particle motion and drift

shells will be enhanced over that familiar from terrestrial studies which show such other important phenomena as longitudinal variations in the loss cones.

It had been noted on Pioneer 10 (Fillius and McIlwain, 1974; Simpson et al., 1974; Trainor et al., 1974), that near the periapsis of the trajectory, there was a reduction in some of the detector count rates which could not be explained by the then available D_2 model of the Jovian magnetic field. With the observations of the broader range of sweeping associated with the satellite Amalthea in the more complex magnetic field model O_3 it was then suggested (Fillius et al., 1975) that probably the strange behavior observed on Pioneer 10 was associated with the sweeping effects of Amalthea. Presented in Figure 7 is the Pioneer 10 trajectory L shell parameter which shows that indeed Pioneer 10 periapsis was within $\sim 0.18\ R_J$ from the simple geometric sweeping region associated with Amalthea when using the O_4 model.

The interpretation of satellite sweeping effects using only the L shell parameter is a rather more simplified approximation than justified in the case of Jupiter. The complete study should include a consideration of the mirror point distribution of the particles and additionally, the position of the spacecraft should be presented in B, L space such that associated with each L shell value there exists a corresponding specific field intensity value. The high order moments of the Jovian magnetic field can be expected to contribute to some L shell splitting so that the satellite sweeping regions may be more extended than the simple geometric absorption considered thus far (see review by Roederer, 1972 and references cited therein).

The hemispherical and azimuthal asymmetries of the O_4 field model provide a quantitative confirmation of the speculated source mechanism and locations of periodic escape of particles from the radiation belts of Jupiter into interplanetary space discussed by Hill et al. (1974) and Vasyliunas (1975).

Implications for Planetary Radio Emissions - Prior to direct measurements of the Jovian magnetic field, ground-based radio astronomy had contributed substantially to our understanding of the magnetic field of Jupiter (see review by Carr and Gulkis (1969), and references contained therein). Not only the approximate field magnitude at the equator, 1 to 10 Gauss, was predicted but also the polarity sense of the magnetic field had been established. The most precisely determined parameter had come from the investigation of the modulation of the electric field polarization characteristics of decimetric radio emissions observed from electrons radiating in the synchrotron mode close to the planet, primarily between 1.5 to 4 R_J.

These observations had provided a good estimate of the tilt and longitude of the equivalent dipole magnetic axis of the planet Jupiter (Komesaroff et al., 1970; Berge, 1974), as well as established its rotation rate relative to coordinate systems I and II, defined on the basis of atmospheric observations. The variation of polarization and its intensity, however, could not be accurately matched to that of any simple dipole and it was suggested that non dipolar contributions were responsible (Conway and Stannard, 1972). Figure 8 shows the shape of the charged particle equator determined from O_4 as observed at different radial distances and illustrates clearly that this, the principal region of emissions, deviates significantly from a simple flat planar geometry.

The latitude variation of the charged particle equator is by no means a simple sinusoid, although at all distances from 1 to 6 R_J, the curves show a minimum latitude near $\lambda_{III} = 225^\circ$. This value determines the longitude of the equivalent dipole and Figure 8 includes the extrapolated values from Berge (1974) and Mead (1974). The variations in the peak-to-peak excursions of these curves also suggest a reasonable explanation for the various differences in derived magnetic field characteristics associated with separate studies of the decimetric emission at different wavelengths. Since the principal contributions to the different wavelength regions will originate from different regions of the radiation belts, their differing geometrical characteristics will be reflected accordingly into the radiated emissions by their respective positions.

The modulation of the decametric radio emission by the satellite Io has been an enigmatic phenomenon studied in recent years. Based upon the octupole model O_4, Figure 9 presents the position of the Io associated flux tube as seen from the north zenographic pole. The field lines which thread Io, as the satellite moves zenographic longitude, are identified as Io's position varies from 0 to 360°. A comparison of this figure with Figure 4 shows that the northern footprint of Io passes directly over the polar regions of the planetary field. Thus it seems reasonable to speculate that the magnetic field geometry and associated Io flux tube support the idea that the decametric emission is associated with particle precipitation into the auroral regions of the planet.

Much further study is necessary to elaborate more fully on the implications of the magnetic field measurements by the GSFC FGM with

respect to decimetric and decametric radio emissions. Combined with definitive measurements of the distribution functions of charged particles, it should be possible to affect comparisons of the ground-based observations with those predicted from in situ models currently under development.

Some attempts to reconcile the Io footprint and flux tube geometry with decametric observations have been made (Alexander and Smith, private communication). The limited data set of Pioneer 11 does not permit determination of higher order multipoles than in O_4 and it is felt that the field geometry within 0.5 R_J of the surface and at the surface of Jupiter may not be sufficiently accurately determined to yield completely satisfactory results in any such studies.

Implications: Planetary Interiors - The most plausible source mechanism of planetary magnetism is thought to be a dynamo operating in the interior and most probably driven by a convection process (Busse, 1975; Gubbins, 1974; Soward and Roberts, 1975). The significant higher order moments can be interpreted as representing two different phenomena associated with the planetary field. The first is the displacement of the equivalent dipole center from the center of the planet, which yields quadrupole and higher order terms when the field is described by a centered harmonic expansion. This mathematical artifact can be removed by an expansion centered on the displaced dipole position, the magnitude and direction of the displacement determined from the centered quadrupole terms so as to reduce to zero the three terms g_{20}, g_{21} and h_{21}. The remaining quadrupole terms g_{22} and h_{22} have to do with "warping" of the magnetic equator. When this is done, the remaining quadrupole and octupole

moments given an indication of the proximity of the source region generating the magnetic field to the surface of the planet. A preliminary calculation based on a spherical harmonic expansion of order n = 3 (internal terms up to octupole) yields offset quadrupole and octupole moments which are 6.2% and 19% of the dipole moment respectively. The corresponding values for Earth are 6.25% and 9.9% respectively (Hilton and Schulz, 1973). On the basis of this preliminary calculation no definitive statements can be made about the relative size of the source regions at Earth and Jupiter. Since the octupole may not be accurately determined due to the limited data set imposed by the Pioneer 11 trajectory, it is only possible to speculate that these source regions are similar in relative size, the main difference between the two planets being that in the case of Jupiter there is apparently a larger equivalent dipole displacement from the center (0.12 R_J vs. 0.063 R_E).

Further studies comparing Earth and Jupiter's planetary fields will be exploited to provide more precise insight on the mechanisms of planetary magnetic dynamos. The solar dynamo appears to be related to a more dynamic process and thus comparison with multipolar representations of the solar field are sensitive to the specific solar period of interest.

Summary - The main magnetic field of Jupiter, as measured by the GSFC FGM on Pioneer 11, is found to be more complex than indicated by Pioneer 10 helium vector magnetometer results. At distances less than 3 R_J, the magnetic field is observed to increase more rapidly than an inverse cubed distance law associated with any simple dipole model. Contributions from higher order multipoles are significant, with the quadrupole and octupole being 24% and 21% of the dipole moment respectively.

Because the data set is not uniformally distributed over a surface enclosing the planet, cross coupling exists in the determination of coefficient sets depending upon the maximum order of the multipole considered. For the GSFC octupole model O_4 the dipole term is found to have a moment of $4.28 \pm .15$ Gauss R_J^3 tilted $9.6^\circ \pm 0.3^\circ$ towards system III longitude of $232 \pm 3^\circ$. Considerable hemispherical and azimuthal asymmetry of the magnetic field is found with maximum field intensities of 14 Gauss in the northern polar regions and 10.4 Gauss in the southern polar region.

The deviation of the main planetary magnetic field from a simple dipole leads to distortion of the charged particle L shells and warping of the magnetic equator. Enhanced absorption effects associated with the satellites Io and Amalthea are predicted as a result and the O_4 model provides better agreement with the observed absorption effects at Amalthea as reflected in the multiple peak structure of the radiation belts close to the planet. These effects are consistent with the conclusions derived from many years of decimetric and decametric radio emissions regarding characteristics of the planetary field. The magnitude of the higher order moments described in an offset dipole coordinate system, suggest that the relative sizes of the source regions generating the field at Jupiter and Earth are of comparable magnitude.

Acknowledgments - We appreciate the outstanding efforts and the prompt processing and analysis of these data by F. W. Ottens and R. F. Thompson of the NASA/GSFC. Important discussions of these results with our colleagues, in particular J. K. Alexander, S. M. Gulkis, J. Warwick, J. Van Allen, R. W. Fillius and J. Roederer are appreciated. The L shell

values are provided as the initial result of a collaborative effort with Dr. J. Roederer of the University of Denver, to study the motion of charged particles in the magnetosphere of Jupiter.

TABLE I (West Longitude III)

	Dipole	OTD	Quadrupole	Octupole
Moment (Gauss R_j^3)	4.36	4.35	4.36	4.28
Tilt	8.41°	9.52°	9.83°	9.6°
Longitude	246°	236°	235°	232°
Vector RMS (Gauss)	0.021	0.0113	0.0106	0.0085
Condition Number	--	--	--	50

TABLE II (+East Longitude III)

		Quadrupole		Octupole (O_4)	
n	m	C_n^m	ϕ_n^m	C_n^m	ϕ_n^m
1	0	4.298		4.218	
1	1	0.745	+125°	0.715	+128°
1	-	4.36	(100%)*	4.28	(100%)*
2	0	-0.233		-0.203	
2	1	0.527	+172°	0.872	+182°
2	2	0.246	-26°	0.521	-25°
2	-	0.627 ($=M_n$)	(14.4%)	1.036	(24.2%)
3	0			-0.233	
3	1			0.585	-128°
3	2			0.515	+5°
3	3			0.374	+47°
3	-			0.895	(20.9%)

$$\phi_n^m = \frac{1}{m} \arctan \left[\frac{h_n^m}{g_n^m} \right]$$

$$C_n^m = \left[(g_n^m)^2 + (h_n^m)^2 \right]^{\frac{1}{2}}$$

$$M_n^2 = \sum_{m=0}^{n} (g_n^m)^2 + (h_n^m)^2$$

*by definition

FIGURE CAPTIONS

Figure 1 The complete GSFC triaxial fluxgate magnetometer on Pioneer 11 including 10 bit A-D converter but without external case. The small size is illustrated by the standard size connector. One of the two orthogonally mounted cores is shown with two orthogonal sense windings. There is redundancy in the sensing and readout of the Z-axis field component by the two cores.

Figure 2 Comparison of Z-axis component magnetic field data from the A core (Z) using the 10 bit A-D converter of the instrument with the redundant B core (RZ) using the 6 bit A-D converter of the Pioneer 11 spacecraft. Solid curves are preflight and corrected calibrations.

Figure 3 Comparison plot of spherical coordinate components of the GSFC-FGM magnetic field measured on Pioneer 11 with the GSFC O_4 model.

Figure 4 Isointensity contour maps of the main field of Jupiter at the surface of the planet (assuming 1/15.4 flattening) and at 2 R_J for the O_4 model.

The trace of the Pioneer 11 trajectory is shown in the upper panel, as is the trace of the footprint of the Io associated flux tube.

Figure 5 Comparison of the derived L shell parameter for the O_4, D_2 and Randall models along the Pioneer 11 trajectory. The L values are computed for charged particles which mirror at the spacecraft, i.e., a local pitch angle of 90°.

Indicated regions of absorption effects due to the natural satellites Io and Amalthea are identified for the O_4 and Randall models.

Figure 6 Comparison of electron and proton fluxes measured by the UCSD experiment (Fillius et al., 1975) near closest approach to Jupiter by Pioneer 11 illustrating a multiple peak structure with the predicted times of absorption due to Amalthea and the crossing of the charged particle equator (EQ).

Figure 7 Same as Figure 5 but for Pioneer 10 trajectory. Note that Pioneer 10 came to within 0.18 R_J of Amalthea's geometrical sweeping region.

Figure 8 Latitude vs. longitude plot of minimum B intensity along a field line at various zenocentric distances.

Figure 9 Intersection of field lines threading Io with the surface of Jupiter from the GSFC O_4 model. The zenographic longitude of Io is indicated alongside the individual North-South footprints.

REFERENCES

Acuna, M. H.; and Ness, N. F. 1975a. The Pioneer XI high field fluxgate magnetometer. Space Sci. Inst. 1, 177-188.

Acuna, M. H.; and Ness, N. F. 1975b. Jupiter's main magnetic field measured by Pioneer 11. Nature 253: 327-328.

Berge, G. L.; 1974. The position and stokes parameters of the integrated 21 cm radio emission of Jupiter and their variation with epoch and central meridian longitude. Astrophys. J. 191: 775-784.

Busse, F. H.; 1975. A model of the Geodynamo. Geophys. J. Roy. Astr. Soc., in press.

Carr, T. D.; and Gulkis, S. 1969. The magnetosphere of Jupiter. Ann. Revs. Astron. Astrophys. 7: 577-618.

Conway, R. G.; and Stannard, D. 1972. Non-dipole terms in the magnetic fields of Jupiter and the Earth. Nature 239: 142-143.

Fillius, R. W.; McIlwain, C. E.; and Mogro-Campero, Antonio. 1975. Radiation belts of Jupiter: A second look. Science 188: 465-467.

Fillius, R. W.; and McIlwain, C. E. 1974. Measurements of the Jovian Radiation Belts. J. Geophys. Res. 79: 3589-3599.

Gubbins, D.; 1974. Theories of the geomagnetic and solar dynamo. Revs. Geophys. and Space Phys. 12: 137-154.

Hess, W. N.; Birmingham, T. J.; and Mead, G. D. 1974. Absorption of trapped particles by Jupiter's moons. J. Geophys. Res. 79: 2877-2880.

Hill, T. W.; Carbary, J. F.; and Dessler, A. J. 1974. Periodic escape of relativistic electrons from the Jovian magnetosphere. Geophys. Res. Letters. 1: 333-336.

Hilton, H. H.; and Schulz, M. 1973. Geomagnetic potential in offset dipole coordinates. J. Geophys. Res. 78: 2324-2330.

Kaiser, M. L.; and Alexander, J. K. 1972. The Jovian decametric rotation period. Astrophys. Letters 12: 215-217.

Komesaroff, M. M.; Morris, D.; and Roberts, J. A. 1970. Circular polarization of Jupiter's decimetric emission and the Jovian magnetic field strength. Astrophys. Letters 7: 31-36.

McIlwain, C. E.; and Filliuz, R. W. 1975. Differential spectra and phase space densities of trapped electrons at Jupiter. J. Geophys. Res. 80: 1341-1345.

Mead, G. D.; 1974. Pioneer 10 mission: Jupiter encounter. J. Geophys. Res. 79: 3514-3521.

Mead, G. D.; and Hess, W. N. 1973. Jupiter's radiation belts and the sweeping effect of its satellites. J. Geophys. Res. 78: 2793-2811.

Roederer, J. G.; 1972. Geomagnetic field distortions and their effects on radiation belt particles. Revs. Geophys. and Space Phys. 10: 599-630.

Schulz, M.; 1974. Geomagnetically trapped radiation. SAMSO Report TR-74-264.

Simpson, J. A.; Hamilton, D. C.; McKibben, R. B.; Mogro-Campero, A.; Pyle, K. R.; and Tuzzolino, A. J. 1974. The protons and electrons trapped in the Jovian dipole magnetic field region and their interaction with Io. J. Geophys. Res. 79: 3522-3544.

Smith, E. J.; Davis, L. Jr.; Jones, D. E.; Coleman, P. J.; Colburn, D. S.; Dyal, P.; Sonett, C. P.; and Frandsen, A. M. A. 1974. The planetary magnetic field and magnetosphere of Jupiter: Pioneer 10. J. Geophys. Res. 79: 3501-3513.

Smith, E. J.; Davis, L. Jr.; Jones, D. E.; Coleman, P. J. Jr.; Colburn, D. S.; Dyal, P.; and Sonett, C. P. 1975. Jupiter's magnetic field, magnetosphere and interaction with the solar wind: Pioneer 11. Science 188: 451-455.

Soward, A. M.; and Roberts, P. H. 1975. Recent developments in dynamo theory. Ann. Rev. Fluid Mech. 7: in press.

Trainor, J. H.; McDonald, F. B.; Teegarden, B. J.; Webber, W. J.; and Roelof, E. C. 1974. Energetic particles in the Jovian magnetosphere. J. Geophys. Res. 79: 3600-3613.

Trainor, J. H.; McDonald, F. B.; Stillwell, D. E.; Teegarden, B. J.; and Webber, W. J.; 1975. Jovian protons and electrons: Pioneer 11. Science 188: 462-465.

Van Allen, J. A.; Baker, D. N.; Randall, B. A.; and Sentman, D. D. 1974. The magnetosphere of Jupiter as observed with Pioneer 10 1. Instrument and principal findings. J. Geophys. Res. 79: 3559-3577.

Van Allen, J. A.; Randall, B. A.; Baker, D. N.; Goertz, C. K.; Sentman, D. D.; Thomsen, M. F.; and Flindt, H. R. 1975. Pioneer 11 observations of energetic particles in the Jovian magnetosphere. Science 188: 459-462.

Vasyliunas, V. M.; 1975. Modulation of Jovian interplanetary electrons and the longitude variation of decametric emissions. Geophys. Res. Letters. 2: 87-88.

West, H. I., Jr.; 1975. Advances in magnetospheric physics 1971-1974. Revs. Geophys. Space Physics 13: in press.

Figure 1

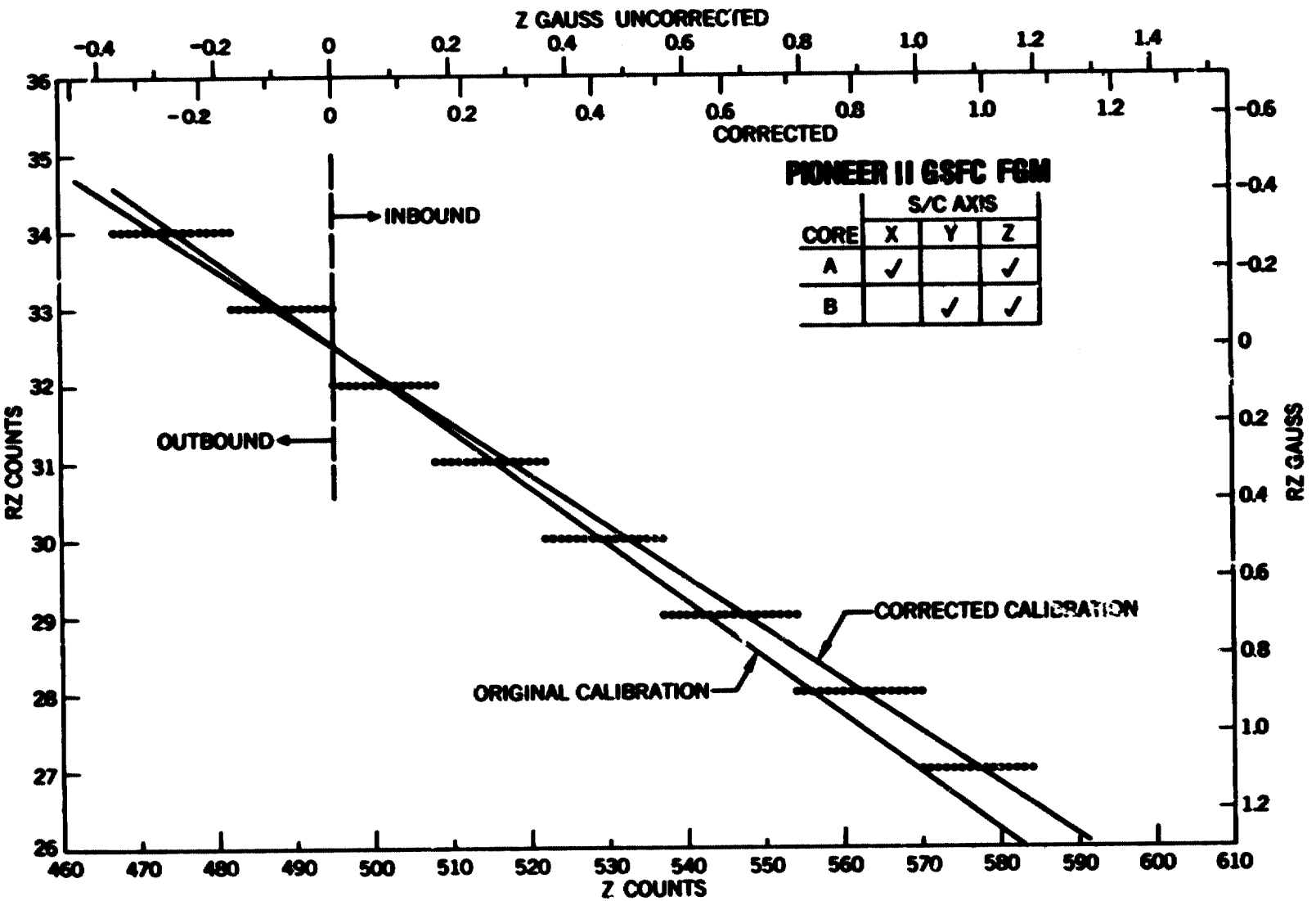
Z GAUSS UNCORRECTED
-0.4
-0.2
0
0.2
0.4
0.6
0.8
1.0
1.2
1.4
CORRECTED
PIONEER II GSFC FGM
S/C AXIS
CORE
X
Y
Z
A
B
INBOUND
OUTBOUND
RZ COUNTS
RZ GAUSS
CORRECTED CALIBRATION
ORIGINAL CALIBRATION
Z COUNTS
26
27
28
29
30
31
32
33
34
35
36
460
470
480
490
500
510
520
530
540
550
560
570
580
590
600
610

FIGURE 2

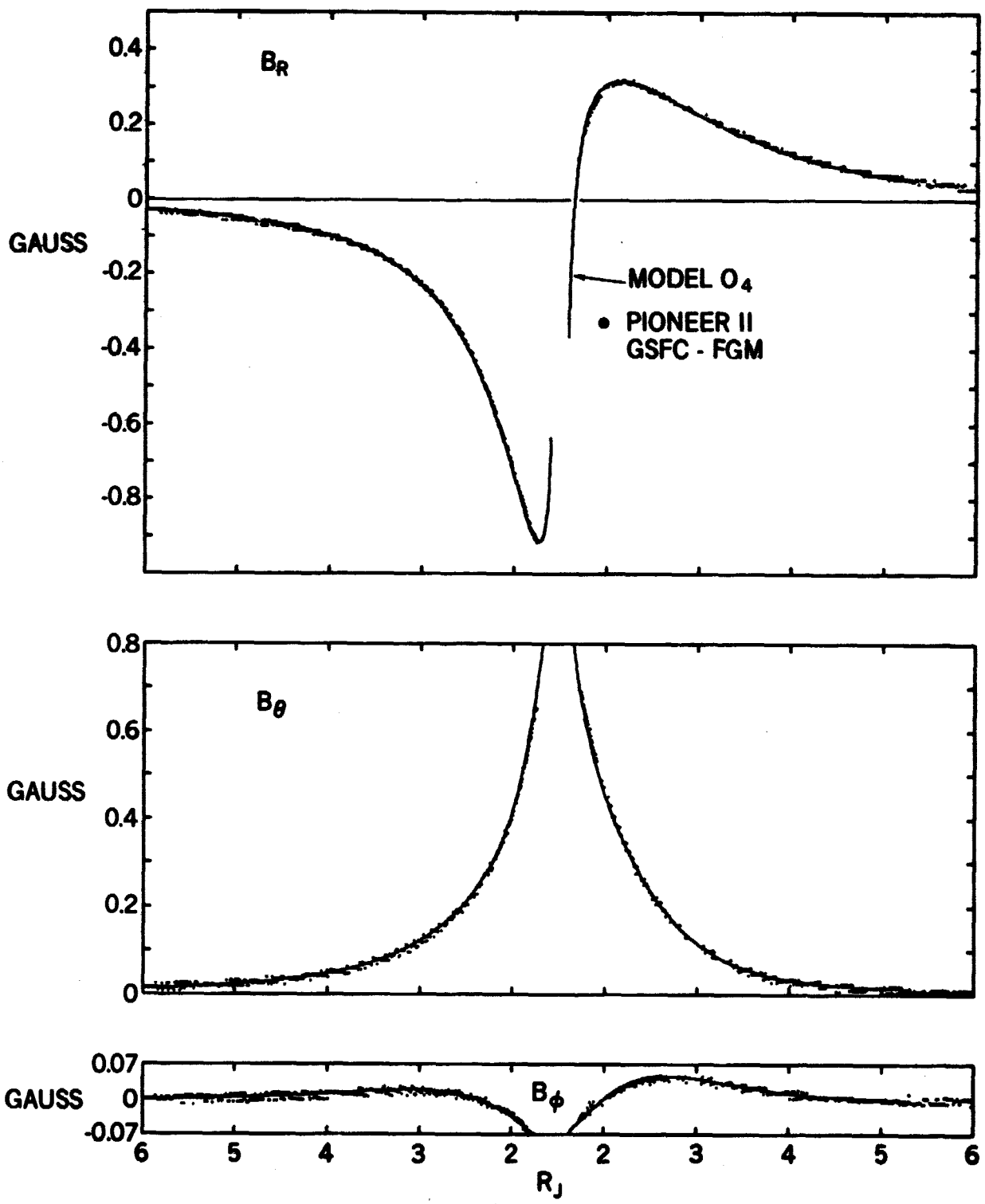
0.4
0.2
0
-0.2
-0.4
-0.6
-0.8
GAUSS
B_R
MODEL O_4
• PIONEER II
GSFC - FGM
0.8
0.6
0.4
0.2
0
GAUSS
B_θ
0.07
0
-0.07
GAUSS
B_ϕ
6
5
4
3
2
2
3
4
5
6
R_J

FIGURE 3

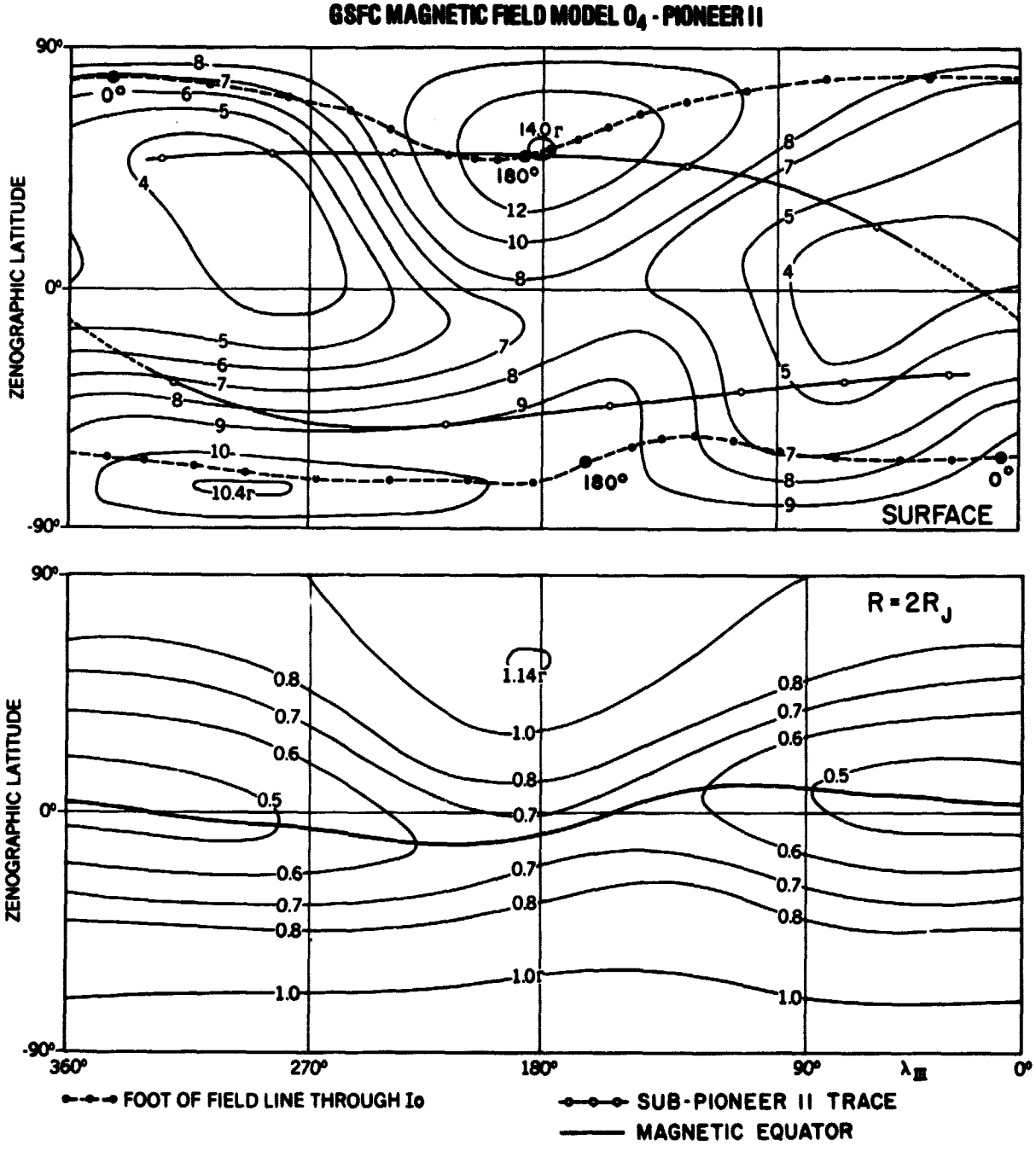
GSFC MAGNETIC FIELD MODEL O_4 - PIONEER II
ZENOGRAPHIC LATITUDE
90°
0°
-90°
SURFACE
14.0r
10.4r
180°
0°
R = 2R_J
1.14r
360°
270°
180°
90°
0°
λ_III
FOOT OF FIELD LINE THROUGH Io
SUB-PIONEER II TRACE
MAGNETIC EQUATOR

FIGURE 4

PIONEER 11 TRAJECTORY AT JUPITER

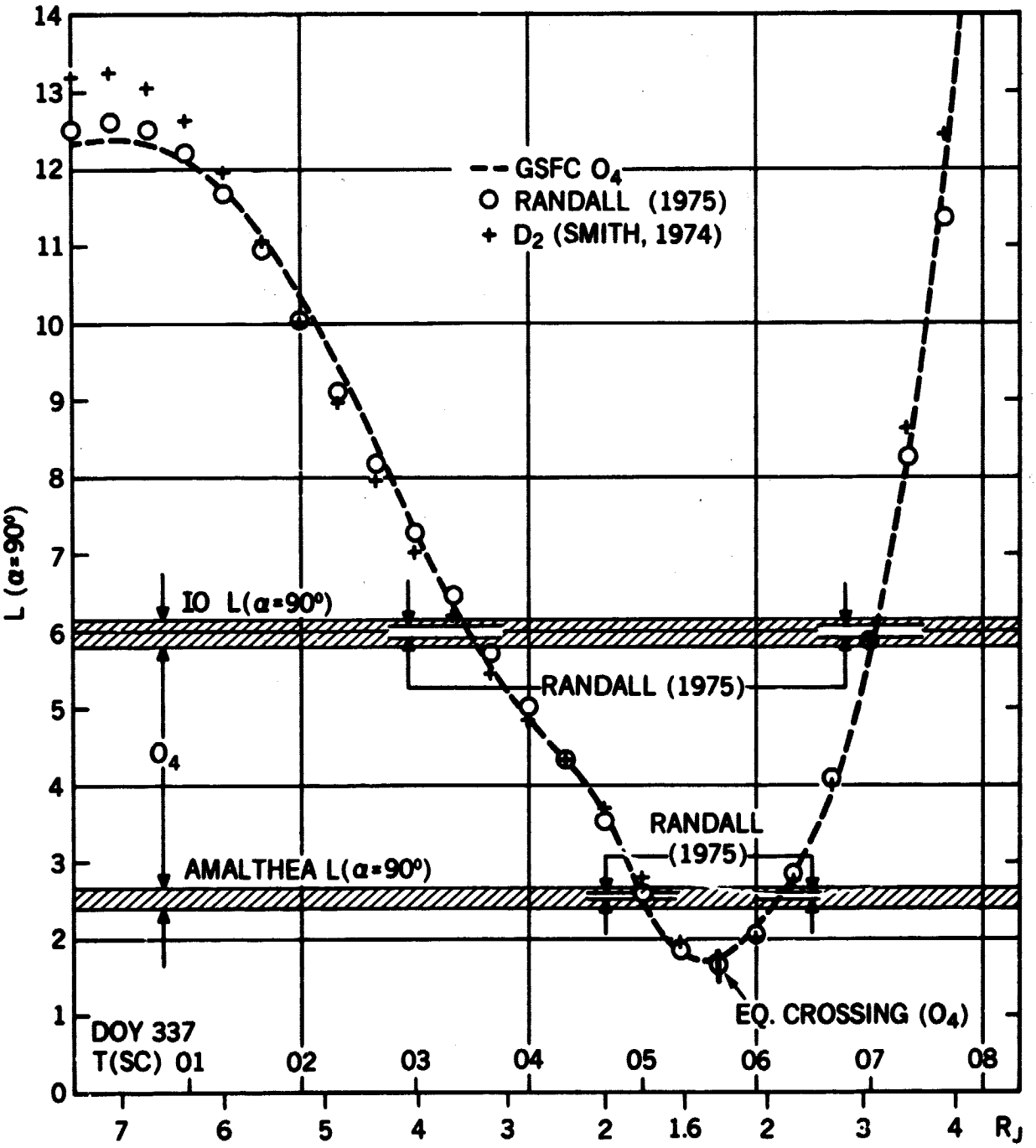

FIGURE 5

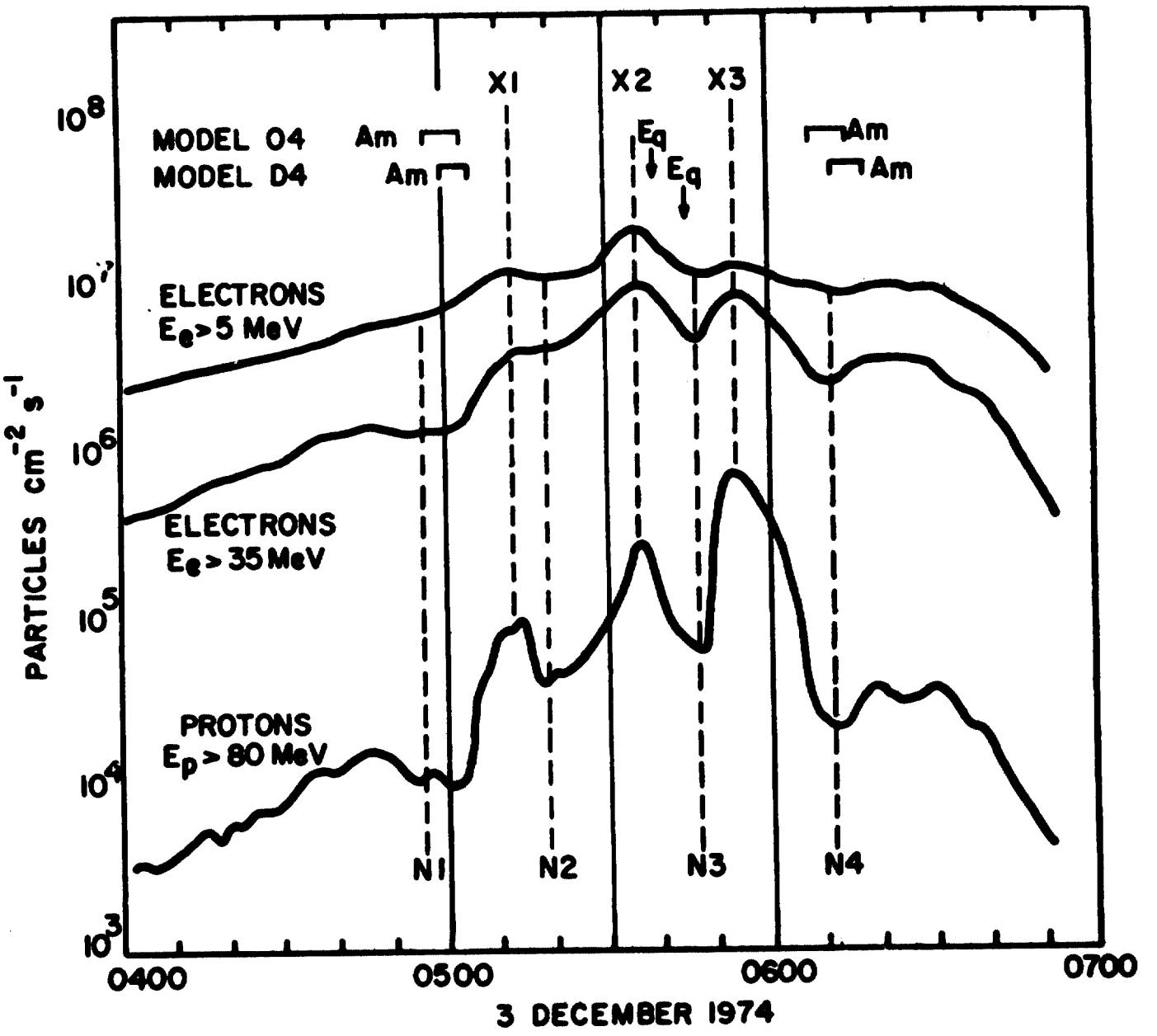
MODEL 04
MODEL D4
Am
Am
X1
X2
X3
Eq
Eq
Am
Am
ELECTRONS
Ee>5 MeV
ELECTRONS
Ee>35 MeV
PROTONS
Ep>80 MeV
PARTICLES cm-2 s-1
10^8
10^7
10^6
10^5
10^4
10^3
N1
N2
N3
N4
0400
0500
0600
0700
3 DECEMBER 1974

FIGURE 6

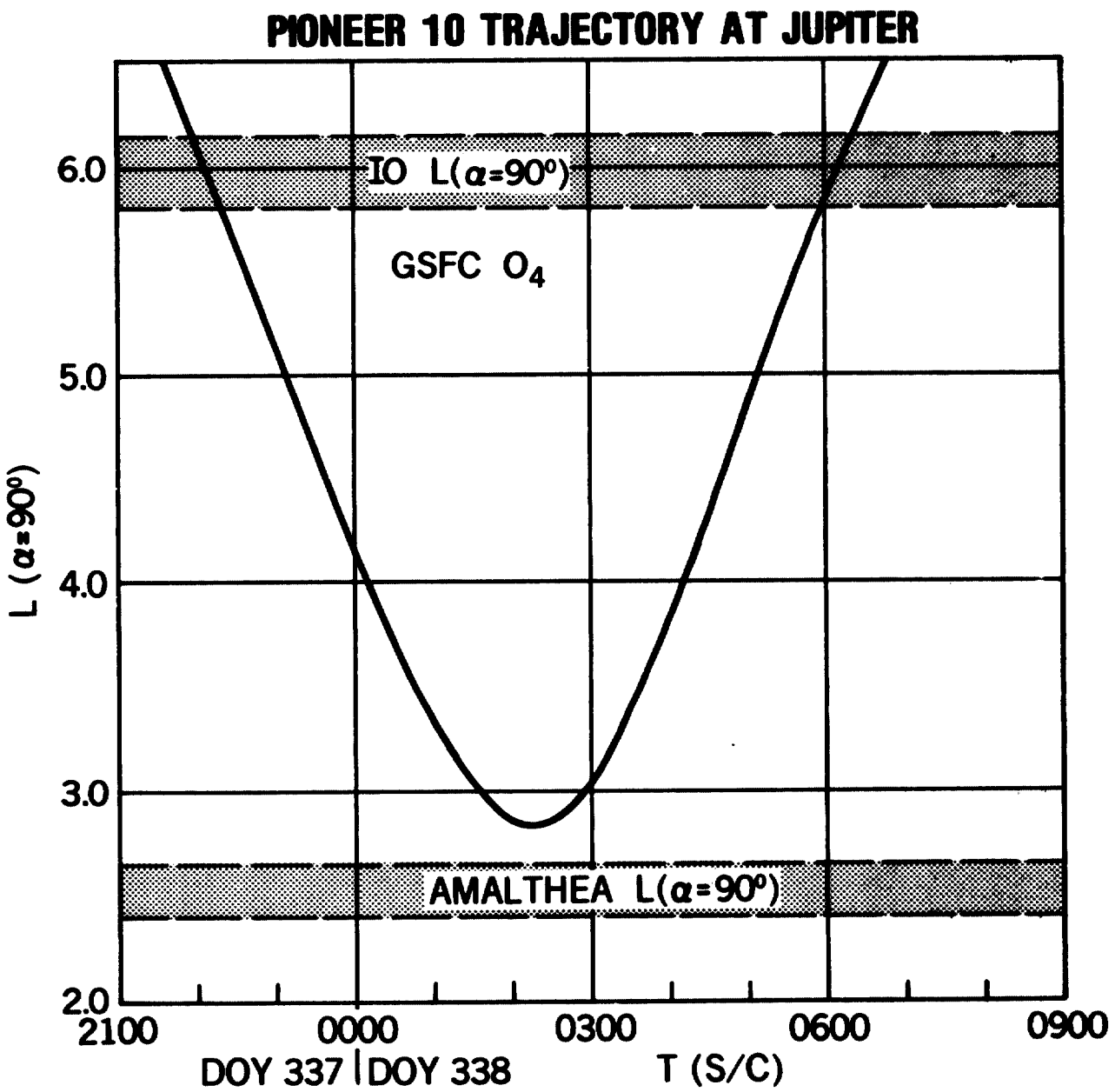
PIONEER 10 TRAJECTORY AT JUPITER
IO L(α=90°)
GSFC O4
AMALTHEA L(α=90°)
L (α=90°)
6.0
5.0
4.0
3.0
2.0
2100
0000
0300
0600
0900
DOY 337
DOY 338
T (S/C)

FIGURE 7

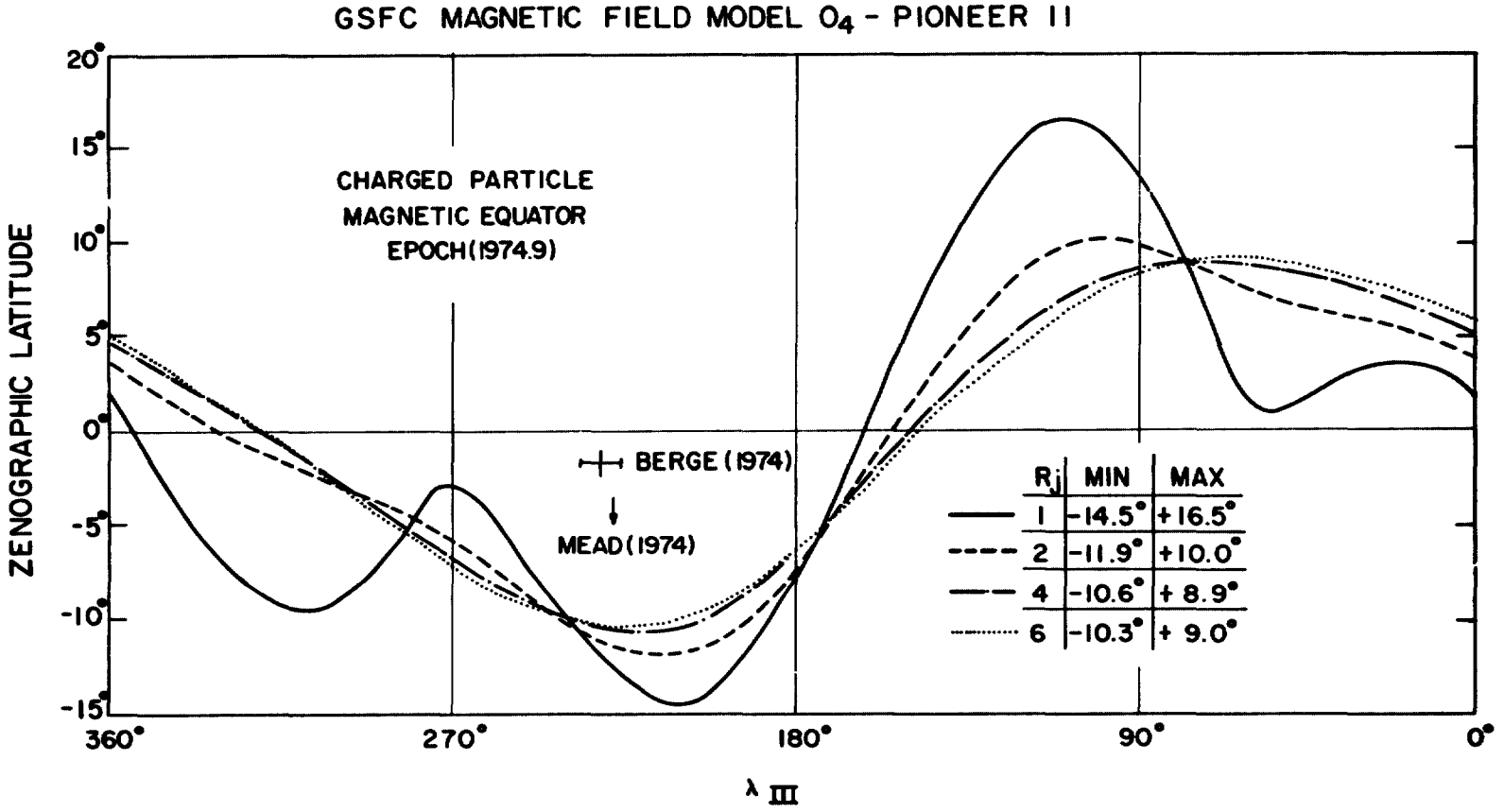
GSFC MAGNETIC FIELD MODEL O_4 - PIONEER 11
CHARGED PARTICLE
MAGNETIC EQUATOR
EPOCH(1974.9)
BERGE (1974)
MEAD(1974)
ZENOGRAPHIC LATITUDE
20°
15°
10°
5°
0°
-5°
-10°
-15°
360°
270°
180°
90°
0°
λ III
Rj | MIN | MAX
1 | -14.5° | +16.5°
2 | -11.9° | +10.0°
4 | -10.6° | + 8.9°
6 | -10.3° | + 9.0°

FIGURE 8

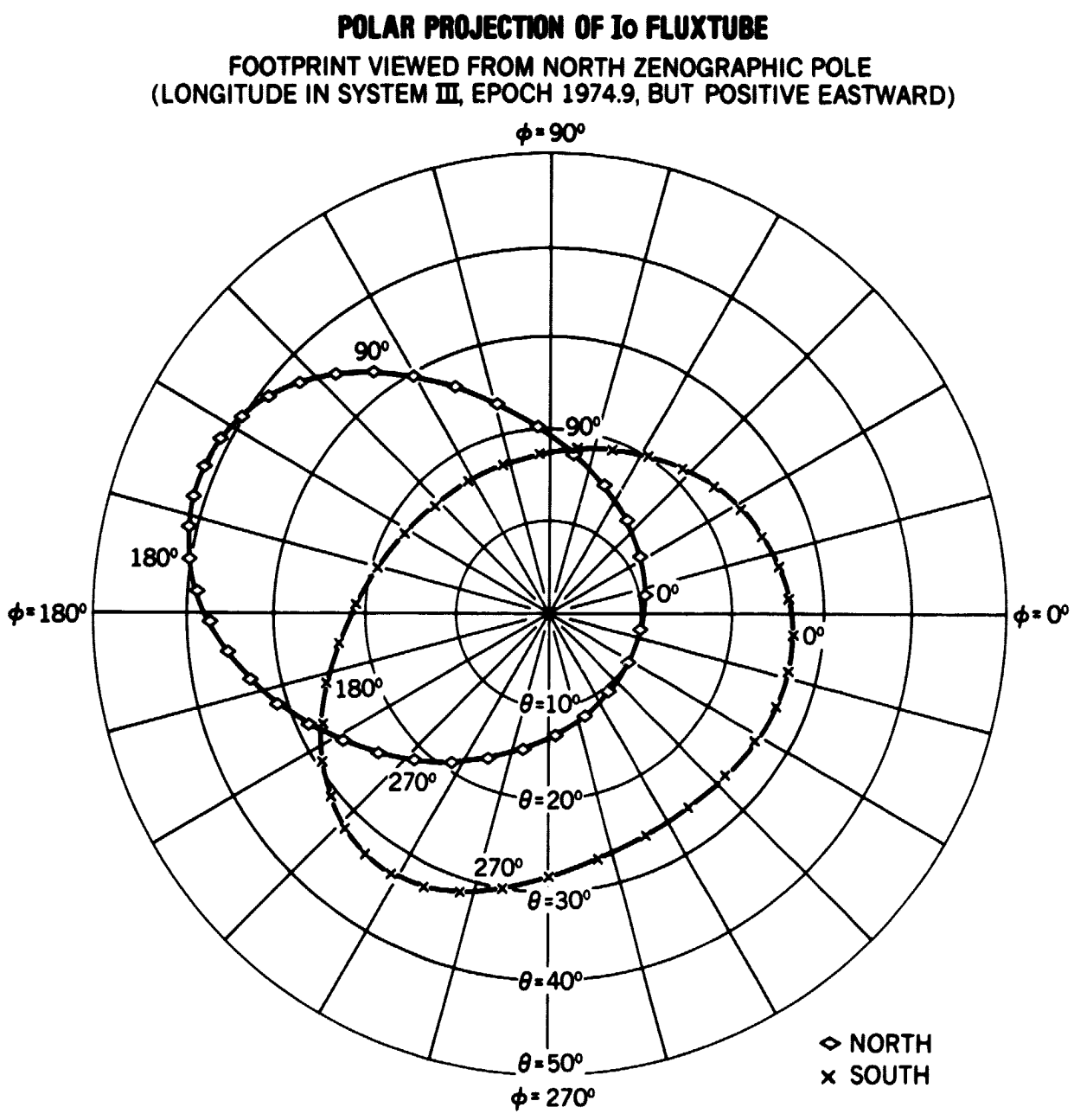
POLAR PROJECTION OF Io FLUXTUBE
FOOTPRINT VIEWED FROM NORTH ZENOGRAPHIC POLE
(LONGITUDE IN SYSTEM III, EPOCH 1974.9, BUT POSITIVE EASTWARD)
φ = 90°
90°
90°
180°
0°
φ = 180°
φ = 0°
0°
180°
θ = 10°
270°
θ = 20°
270°
θ = 30°
θ = 40°
θ = 50°
φ = 270°
θ VS φ
◇ NORTH
× SOUTH

FIGURE 9